Published by :
http://www.ijert.org

International Journal of Engineering Research & Technology (IJERT)
ISSN: 2278-0181
Vol. 7 Issue 07, July-2018

Aerodynamic Study of the Effects of Side-mounted Active Aerodynamic Surfaces

on the Tesla Model S

Yagnavalkya S Mukkamala
Professor,
Department of Automotive Engineering, School of Mechanical Engineering (SMEC)
VIT Vellore, Tamil Nadu, India.

Zia Ahmad Ansari
Fourth year B.Tech. Mechanical Engineering,
School of Mechanical Engineering (SMEC)
VIT Vellore, Tamil Nadu, India.

Anand Vijayaraghavan
Fourth year B.Tech. Mechanical Engineering,
School of Mechanical Engineering (SMEC)
VIT Vellore, Tamil Nadu, India.

***Abstract*— The present work aims to use active aerodynamic surfaces mounted on either side of a car to improve its high speed cornering ability. Actuating individually, they can generate increased drag force on the inboard side of the car while cornering, thus generating a moment about the yaw axis. Further, actuating together, they can be used as air brakes. The simulation of cornering flow is done using a domain characterizing the flow over a car through a typical racetrack corner. Results show that the significant of moment generated about the yaw axis at high speeds is enough to have an impact on the car's cornering ability.**

***Keywords*— Cornering flow; Yaw moment; CFD; Active aerodynamics; Tesla Model S**

I. INTRODUCTION

Active aerodynamics has become a matter of interest in recent years for supercar and hyper car manufacturers. Recent iterations of their designs tend to incorporate active aerodynamic surfaces be it for performance or aesthetics. Recent examples include the active underbody panels of the Porsche 918 and the active body mounted surfaces on the Pagani Huayra for improved road holding [1]. This has also sparked designers to come up with numerous concepts incorporating such surfaces.

This work aims to test the feasibility and effectiveness of such aerodynamic surfaces through flow simulation using CFD. Ansys Fluent has been used to run the simulations for this work. Simulating cornering flow effectively was a must for these simulations. In this work, a custom mesh was used to simulate flow over a Tesla Model S through a typical cornering situation with and without the modifications. Also presented is a comparison of coefficient of moment about the yaw axis between the base and the modified models for a transient case.

II. METHODOLOGY

A. Validation of the Turbulence Model

The turbulence models tested were for the simulations were k-epsilon Standard NWF and k-epsilon Realizable NWF. These models were tested against the Ahmed body with a 25 degree slant angle (CD = 0.289) [3]. Non Equilibrium Wall Functions (NWF) are used instead of standard wall functions because for high Reynolds-number flows such as this, it is not practical to resolve the near-wall region down to the viscous sub layer due to the large number of cells that will be introduced. NWFs are sensitized to pressure gradient effects, and therefore the effects of local variation in thickness of the boundary layer is accounted for [4].

B. Mesh setup and Simulation

The 3D Ahmed body was set up with a surface mesh size of 0.002 m - 0.01 m, with a refining region of mesh size 0.02 m around the body. In addition, there is an inflation layer with 6 layers and first layer height of 0.003 m. The mesh was set up with 1.2 million nodes.

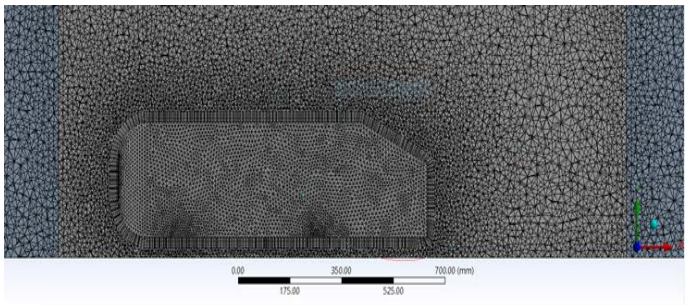

Fig.1 Ahmed body mesh

The given inlet velocity was 40 m/s and the walls were defined with no slip. A steady-state simulation was run for 1000 iterations.

C. Results

TABLE 1

	C_D	Error
Ahmed body (25 degree)	0.2890	-
k-epsilon Standard NWF	0.3050	+5.54%
k-epsilon Realizable NWF	0.2894	+0.14%

The obtained results showed that the k-epsilon Realizable NWF model was more accurate. Therefore, this model was used for future simulations in the present work.

(This work is licensed under a Creative Commons Attribution 4.0 International License.)

International Journal of Engineering Research & Technology (IJERT)
ISSN: 2278-0181
Vol. 7 Issue 07, July-2018

D. Validation of the Base Model

The base model chosen for this study was the Tesla Model S, since its aerodynamic data has been recently published and made available [5]. It was also chosen because its performance is comparable to a standard GTE/GT3 class car and the automotive industry is headed towards electric technology, making our choice future-proof. This work focuses on the exterior modelling and simulation of the car. The simulation has been set up according to best practice guidelines for Ansys Fluent [4].

E. Model Geometry

The model used was a full-scale model created using Autodesk Alias Autostudio. The surface model was then converted to a B-rep model. To convert surfaces to B-rep bodies, all surfaces must be closed and should not be self-intersecting. Minor adjustments were made on the surface geometry to ease meshing.

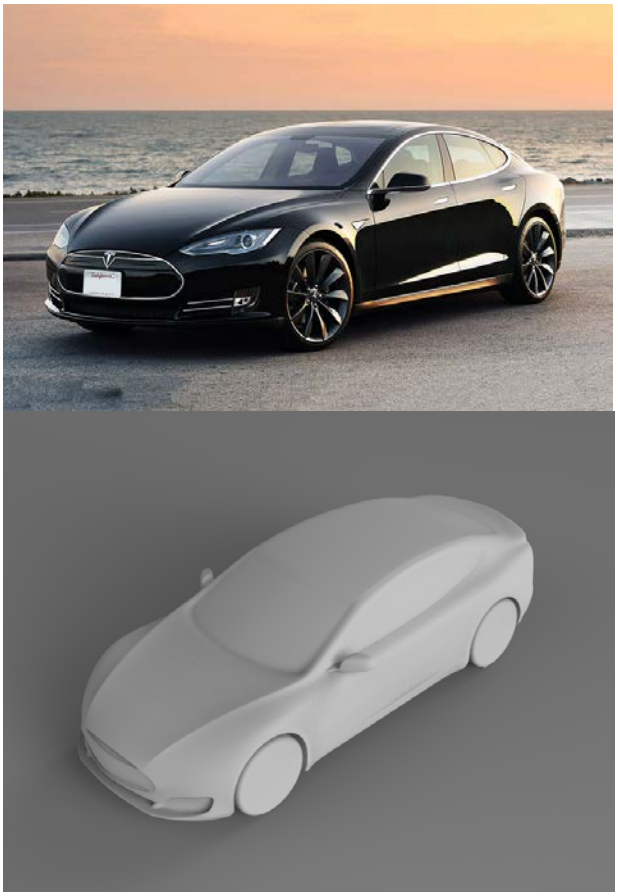

Fig. 2 Real car and Surface model

The contact patch between the road and the tires was made by extrusion, adding a step of 0.01 m, to keep cell skewness low while meshing [6]. The tires were kept as slicks with no rotation and no camber. The ground clearance of the car was 144 mm [5].

F. Mesh setup and Simulation

The model was setup for a half-body simulation with the longitudinal plane as the symmetry plane. The surface mesh size was 0.01 m - 0.04 m, with a refining region having mesh size 0.06 m around the car. The inflation layer was defined with 5 layers using first aspect ratio method. Growth rate of cells was set to 1.04 on all surfaces. The mesh was set up with 2 million nodes.

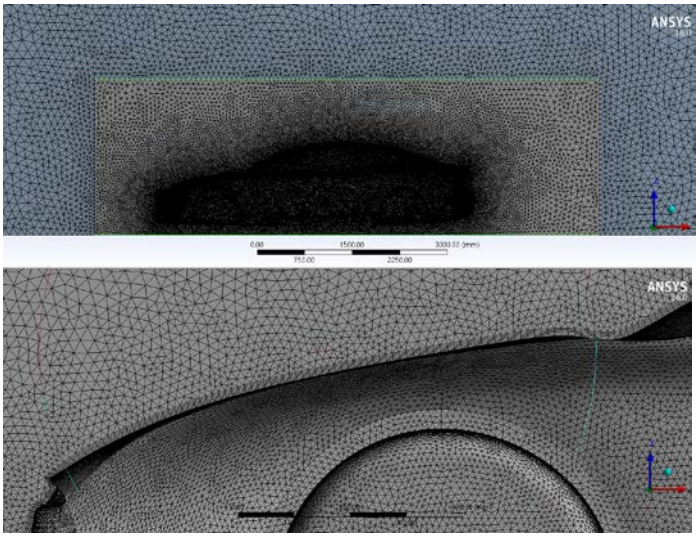

Fig. 3 Mesh and Inflation layer

The inlet velocity was given as 33.33 m/s (120 km/h). A steady state simulation was run for 1000 iterations.

G. Results

Drag force (F_D) = 393.896 N
Frontal area (A) = 2.404 m2
Air density (ρ) = 1.225 N/m3
Velocity (v) = 33.33 m/s

$$C_D = \frac{F_D}{0.5 \times \rho \times v^2 \times A}$$

	C_D	C_L	C_D Error
Results obtained in [5] k-epsilon, slick tires, no rotation	0.2310	0.058	-
Present work	0.2408	0.059	+4.24%

Since the results of the simulation were within 5% of the published results, the base model can be considered validated.

H. Modification

The active aerodynamic surface was added towards the rear of the car, after the rear wheel, where, analytically, the moment generated would be maximum as it is farthest from the yaw axis.

(This work is licensed under a Creative Commons Attribution 4.0 International License.)

International Journal of Engineering Research & Technology (IJERT)
ISSN: 2278-0181
Vol. 7 Issue 07, July-2018

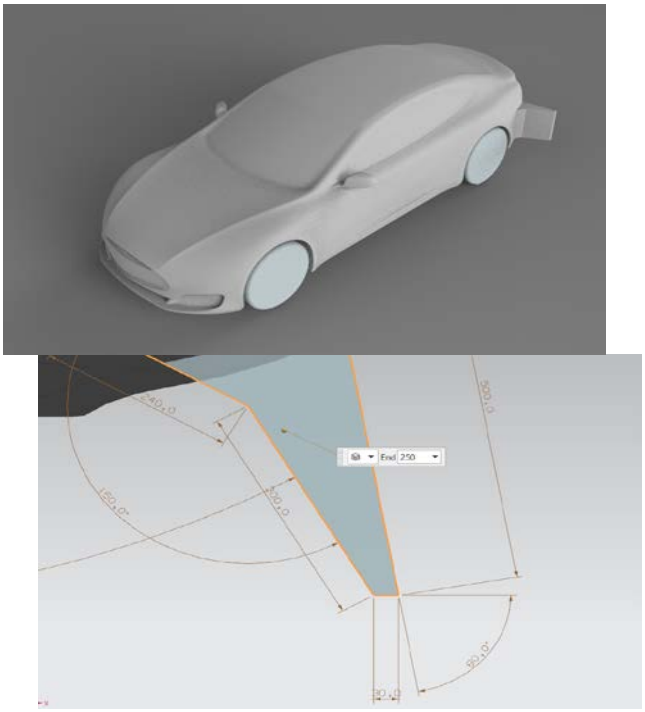

Fig. 4 Modified model and surface dimensions

The surface has dimensions 0.3 m×0.4 m with an effective area of 0.12 m2 angled 30 degrees to the tire axis. In theory, the surface will actuate only while steering and will sit flush with the car's surface otherwise, having no effect on normal driving conditions. The domain was set up for a 15 degree yaw case over a 60 m radius, roughly equal to 12 car-lengths. For the following simulations, tires and suspension have been considered rigid, with no camber.

I. Simulation

The simulation considered the car taking a left turn at 55.55 m/s (200 km/h), over a 60 m radius at a 15 degree yaw rate. In the standard yaw, the onset angle is equal to the angle of yaw. While cornering, the flow onset angle at the front and rear of the car is different [7]. To simulate this, a curved domain was used (Fig. 5) in which there is a constant static pressure along the walls. Mesh and refining region were set up as in the validation study. Steady and transient simulations were performed for the base model as well as the modified model, and coefficient of moment generated by airflow was monitored. The transient simulation was set up for 0.55 seconds with step size of 0.011 seconds.

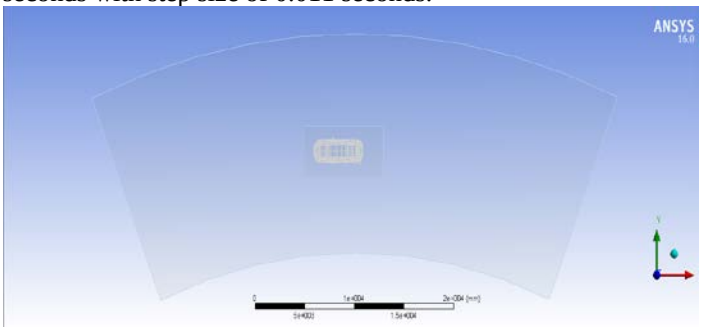

Fig. 5 Cornering flow simulation setup

III. RESULTS AND DISCUSSION

A. Steady-state analysis

	Moment (Nm)	C_Z	C_D	Variation
Base, straight line	0	0	0.2408	-
Base, cornering	-111.196	-0.0588	0.3796	+57.64%
Modified, cornering	432.205	0.2287	0.4390	+82.31%

In the base model, wind resistance creates a clockwise moment of magnitude 114.196 Nm about the yaw axis while cornering. The amount is significant due to the high speed of the car. In the modified case, the moment generated is 432.205 Nm counter-clockwise, with the surface alone generating 300.837 Nm at 55.55 m/s, resulting in a 488.68% increase.

A 57.64% increase in drag is noted for a corner radius of 60 m (12 car-lengths). The increase in drag while cornering is mainly because of the larger area blocking the air, causing higher pressure forces on the inboard side. The flow onset angle at the front and rear are different so the high pressure region is concentrated towards the front. While cornering the vortices and wake become asymmetrical, resulting in formation of a low pressure region towards the rear outboard side. This creates an overall higher pressure difference between the front and rear ends than in a straight-line case. The outboard C-pillar vortices, being stronger, also cause a severe increase in drag. The surface causes a larger wake (Fig. 6), further increasing drag by 15.63%.

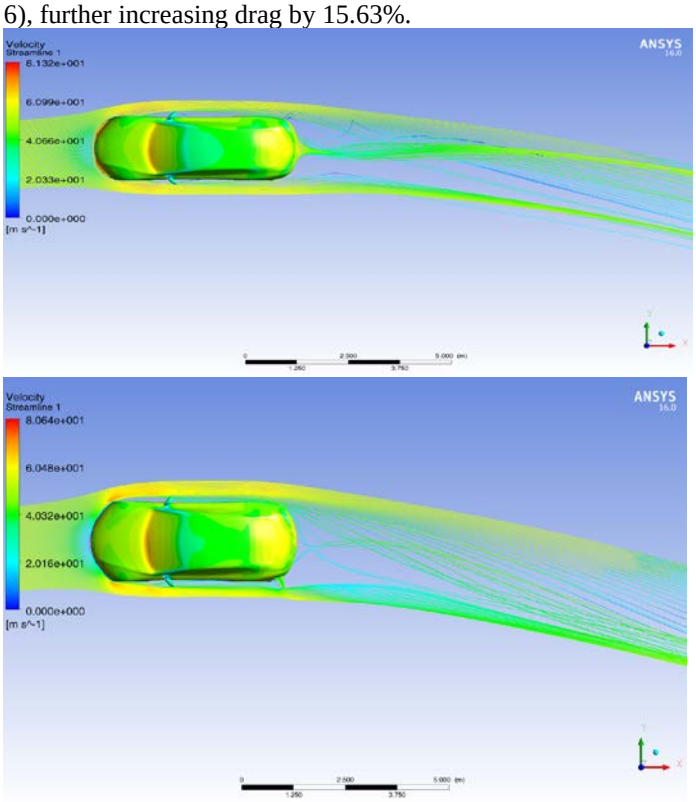

Fig. 6 Velocity streamlines and Pressure contours while cornering: base (left), modified (right)

(This work is licensed under a Creative Commons Attribution 4.0 International License.)

International Journal of Engineering Research & Technology (IJERT)
ISSN: 2278-0181
Vol. 7 Issue 07, July-2018

B. *Transient analysis*

	Moment (Nm) Avg. over time	Max. Moment (Nm)	C_D	Variation With time
Base, cornering	-81.825	623.645 at time 0.33 s	0.3887	< ±10%
Modified, cornering	449.427	1256.739 at time 0.06 s	0.4371	< ±7.5%
% increase	+649.25%	+101.51%	+12.45%	-

C. *Base model*

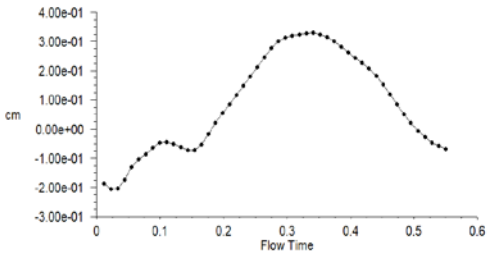

Fig. 7 Coefficient of moment against time

The average yaw moment over time is -81.825 Nm. The moment generated increases to reach a maximum of 623.645 Nm in 0.33 seconds. Initially, the clockwise moment is due to the wind resistance, creating a high pressure region at the inboard front end of the car. With time, a low pressure region is formed at the outboard rear edge of the car. This low pressure region is caused by the air flowing along the rear outboard end being pulled into the wake region behind the car. The pressure on the inboard side being relatively higher, creates a net force at the rear end, causing the counter clockwise moment as seen in the graph above. This effect is better illustrated in Fig. 8 below.

The drag induced is similar to results obtained in the steady-state analysis. It increases by 61.42%. The reason being the high pressure region at the front inboard end and a low pressure region at the rear outboard region creating a pressure difference larger than that in the straight-line case. The drag force has less than 10% variation with time, and is observed to be nearly linear.

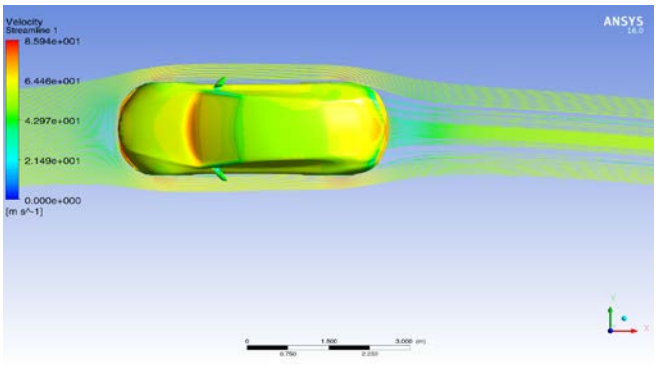

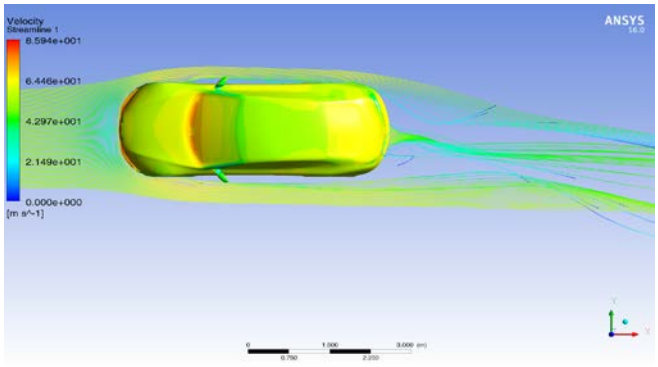

Fig. 8 Variation in flow and pressure with time: 0.02s (left), 0.33s (right)

D. *Modified model*

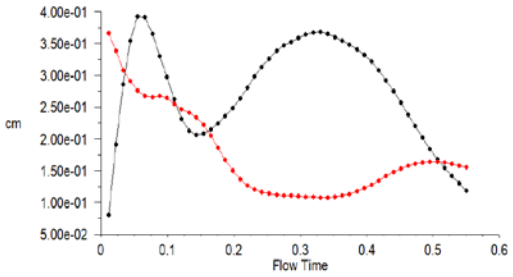

Fig. 9 Coefficient of moment against time: car (•), surface (•)

For the modified model, the average yaw moment over time is 449.427 Nm. The maximum moment generated is 1256.739 Nm at 0.03 seconds. This initial spike in the car's moment coefficient plot (Fig. 9) is due to the same effect as in the base model - formation of a low pressure region due to the air flowing over the rear outboard end being pulled into the wake region behind the car, the larger wake due to the surface contributing to the increased moment generation. However, no clockwise moment is generated in this case.

The drag induced is 81.52% more than the straight-line case. The surface causes a drag increase of 12.54% over the base model cornering case. The variation in drag with time is less than 7.5%, and can be considered nearly linear with time.

The graph also shows the effectiveness of the surface decreasing as the car progresses through the corner till it reaches an effective low. The minor variations during the decrease are due to the variation in the amount of flow incident on the surface caused by flow disturbance caused due to the rear tire. This causes a variation in pressure distribution over the surface, thus having an effect on the moment generated.

(This work is licensed under a Creative Commons Attribution 4.0 International License.)

International Journal of Engineering Research & Technology (IJERT)
ISSN: 2278-0181
Vol. 7 Issue 07, July-2018

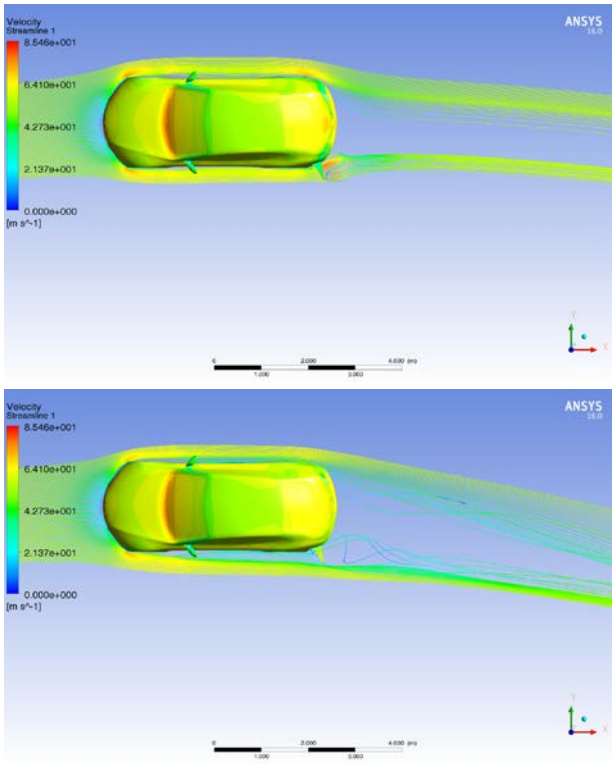

Fig. 10 Variation in flow and pressure with time: 0.02s (left), 0.33s (right)

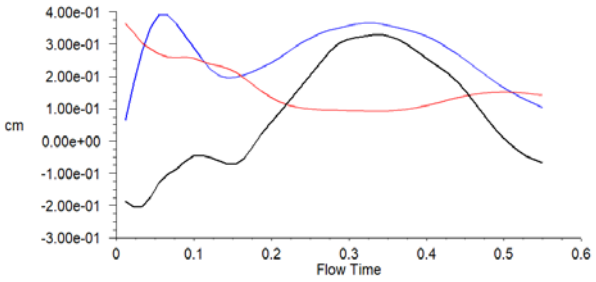

Fig. 11 Coefficient of moment against time: base (•), modified (•), surface (•)

IV. CONCLUSION

In this paper, a Tesla Model S was studied in a case of high speed cornering over a corner radius of 60 m (12 car-lengths) and at a speed of 55.55 m/s (200 km/h). An active aerodynamic surface was then added, and its performance was studied and contrasted against the base model. The base model cornering case had a 57.64% increase in drag over a straight-line case, and adding the surface resulted in a 649.25% increase in yaw moment, from -81.825 Nm to 449.427 Nm, for a 12.54% increase in drag. The surface had significant direct and indirect effects on yaw moment while cornering and an overall increase in yaw moment was observed. An active aerodynamic surface such as this can be retrofitted to a car with sufficient rear overhang, and can be actuated by electro-mechanical or pneumatic actuators. Future studies could be performed on the effects of active aerodynamics on stability of the vehicle, and repurposing such surfaces to increase their functionality.

ACKNOWLEDGEMENT

We would like to express our sincere gratitude to Vellore Institute of Technology, Vellore for providing us with the support and facilities required for the completion of this study.

REFERENCES

[1] M. Corno, S. Bottelli, G. Panzani, M. Tanelli, C. Spelta and S. M. Savaresi, "Improving high speed road-holding using actively controlled aerodynamic surfaces", 2013 European Control Conference (ECC), Zurich, 2013, pp. 1493-1498.

[2] Liu, Yunlong, and Alfred Moser. "Numerical modeling of airflow over the Ahmed body." Air and Climate Group, Swiss Federal Institute of Technology, ETH-Zentrum WET Al (2003).

[3] Timur Dogan, Michael Conger, Dong-Hwan Kim, Maysam Mousaviraad, Tao Xing and Fred Stern, “Simulation of Turbulent Flow over the Ahmed Body”, IIHR-Hydroscience & Engineering, University of Iowa. 2016.

[4] Marco Lanfrit, “Best practice guidelines for handling Automotive External Aerodynamics with FLUENT”, 2005.

[5] Qi-Liang WANG, Zheng WU, Xian-Liang ZHU, Li-Li LIU, Ying-Chao ZHANG, Fu-You JIANG, “Analysis of Aerodynamic Performance of Tesla Model S by CFD”, Proceedings of the 3rd Annual International Conference on Electronics, Electrical Engineering and Information Science (EEEIS 2017), Advances in Engineering Research, 2017, doi:10.2991/eeeis-17.2017.3 .

[6] Diasinos, Sammy, Tracie J. Barber, and Graham Doig. "The effects of simplifications on isolated wheel aerodynamics." Journal of Wind Engineering and Industrial Aerodynamics 146 (2015): 90-101.

[7] James Keogh, Tracie Barber, Sammy Diasinos, Graham Doig, “The aerodynamic effects on a cornering Ahmed body”, Journal of Wind Engineering and Industrial Aerodynamics, Volume 154, 2016, Pages 34-46, ISSN 0167-6105.

[8] Huminic, A. and Huminic, G. (2008), “On the Aerodynamics of the Racing Cars”, SAE Technical Paper 2008-01-0099, doi:10.4271/2008-01-0099.

[9] Ueno, D., Hu, G., Komada, I., Otaki, K. et al. (2006), “CFD Analysis in Research and Development of Racing Car", SAE Technical Paper 2006-01-3646, doi:10.4271/2006-01-3646.

[10] Janson, T. & Piechna, J., “Numerical Analysis of Aerodynamic Characteristics of a of High-Speed Car With Movable Bodywork Elements”, Archive of Mechanical Engineering, 62(4), 2015, pp. 451-476.

[11] Niklas Winkler, Lars Drugge, Annika Stensson Trigell, Gunilla Efraimsson, “Coupling aerodynamics to vehicle dynamics in transient crosswinds including a driver model, In Computers & Fluids, Volume 138, 2016, Pages 26-34, ISSN 0045-7930, doi.org/10.1016/j.compfluid.2016.08.006.

[12] A. Brunn, E. Wassen, D. Sperber, W. Nitsche, F. Thiele, “Active drag control for a generic car model”, R. King (Ed.), Active Flow Control, vol. 95, Springer, Berlin, Heidelberg (2007), pp. 247-259.

(This work is licensed under a Creative Commons Attribution 4.0 International License.)